Characterization of Nucleosomes Consisting of the Human Testis/Sperm-Specific Histone H2B Variant (hTSH2B)†

Andra Li,‡ Allison H. Maffey,‡ Wade D. Abbott,‡ Natalia Conde e Silva,§ Ariel Prunell,§ Joseph Siino,|| Dmitrii Churikov,⊥ Andrei O. Zalensky,⊥ and Juan Ausió*,‡

Department of Biochemistry and Microbiology, University of Victoria, Victoria, British Columbia, Canada V8W 3P6, Institut Jacques Monod, Centre National de la Recherche Scientifique, et Universite Denis Diderot Paris 7, 2 Place Jussieu, 75251 Paris Cedex 05, France, Jones Institute for Reproductive Medicine, East Virginia School of Medicine, Norfolk, Virginia 23507, and Division of Biological Sciences, University of California, Davis, Davis, California 95616

Received September 8, 2004; Revised Manuscript Received November 2, 2004

ABSTRACT: We have reported earlier the occurrence of a specific histone H2B variant in human testis and sperm. Here we have structurally characterized this protein, its association with the rest of the histone octamer, and its effects on the nucleosome structure. We show that a reconstituted octamer consisting of hTSH2B and a stoichiometric complement of histones H2A, H3, and H4 exhibits a lower stability compared to the reconstituted native counterpart consisting of H2B. In contrast, the hTSH2B containing octamers are able to form nucleosome core particles which are structurally and dynamically indistinguishable from those reconstituted with octamers consisting of only native histones. Furthermore, the presence of hTSH2B in the nucleosome does not affect its ability to bind to linker histones.

Replacement histone variants are coming of age as the functional and structural role of several replacement H2A and H3 variants has only recently started being elucidated (*1*, *2*). Histone H2A.X has been the focus of recent attention (*3*, *4*). In its phosphorylated form, it has been shown to play a critical role in DNA repair and in meiosis (*5*−*7*). The functional relevance of histone H2A.Z is underscored by its indispensability for survival in many organisms (*8*), and this variant is currently at the center of controversial structural and functional studies (*9*−*14*). The newest discovered member of the H2A family of variants, macroH2A (*15*), has also been the focus of attention of recent functional and structural work (*12*, *16*−*18*). In a similar fashion, the physiological implications of histone H3.3 have started to unravel in the past few years (*1*). As the functional role of these variants is being clarified, their structural implications still remain largely elusive (*19*).

The structural variation that differentiates replacement core histone variants from their canonical counterparts can affect different regions of the histone molecule to different extents (*2*). For instance, in histone H2A.Z, the main sequence departure takes place at the C-terminal end of the molecule which is the part that has been shown to play a critical role for its indispensability (*8*). MacroH2A contains a large non-histone domain which extends from its C-teminal end (*15*). Histone H3.3 is different from H3.1 and H3.2 in only a few amino acids which mainly affect the histone fold domain of the molecule. CENP-A,[1] a histone variant related to H3 which is part of the centromeric chromatin, exhibits an extensive amount of sequence variation at its N-terminal domain and to a lesser extent throughout the rest of the molecule (*20*). In contrast to H2A and H3, not many histone variants have been characterized for either core histone H2B or core histone H4.

In the course of vertebrate spermatogenesis, the somatic histones which are present at the onset of the differentiation process undergo several transitions. These transitions occur in those organisms in which the main protein chromosomal component consists of protamines in their mature spermatozoa (*21*, *22*). This involves the replacement by different testis-specific histone variants (*6*, *23*, *24*) before they are finally replaced by protamines at the end of spermatogenesis. Human spermatogenesis is rather unique in that the spermatozoa, in addition to a massive protamine presence, retain 10−15% of specific core histone variants (*25*−*27*) with unknown biological function. One such histone (hTSH2B) has recently been characterized (*28*). The main sequence difference between hTSH2B and human somatic H2B occurs at the N-terminal end of the molecule where three of the four proline amino acids that are present in the somatic counterpart of this histone are replaced by phosphorylatable (S/T) amino acids in hTSH2B (see Figure 1 and ref *28*).

In this paper, we report the structural characterization of hTSH2B and of the complexes resulting from its association

†This work was supported by Canadian Institutes of Health Research (CIHR) Grant MOP-57718 to J.A. and by National Institutes of Health Grant HD 39830 to A.O.Z.

* To whom correspondence should be addressed. Phone: 250-721 8863. Fax: 250-721 8855. E-mail: jausio@uvic.ca.

‡ University of Victoria.

§ Centre National de la Recherche Scientifique and Universite Denis Diderot Paris 7.

|| University of California, Davis.

⊥ East Virginia School of Medicine.

[1] Abbreviations: CD, circular dichroism; CENP-A,: centromeric protein A; EDTA, ethylenediaminetetraacetic acid; HPLC, high-performance liquid chromatography; hTSH2B, human testis-specific histone H2B; nNCP, native nucleosome core particles; PAGE, polyacrylamide gel electrophoresis; SDS, sodium dodecyl sulfate.

10.1021/bi048061n CCC: $30.25
Published on Web 01/29/2005

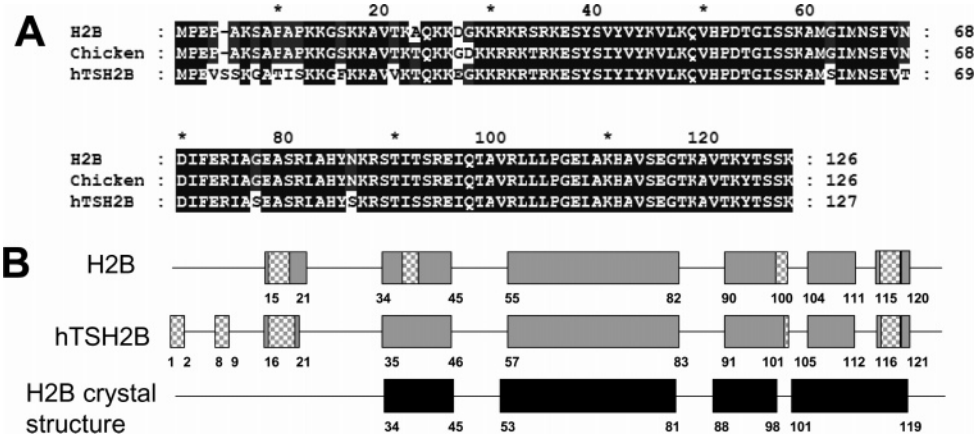

FIGURE 1: (A) Protein sequence comparison of somatic human histone H2B (*59*), chicken histone H2B (*60*), and the human hTSH2B sperm histone variant (*28*). (B) Schematic representation of the secondary structure of the human H2B histone variants. Shown in black are the α-helical regions of H2B determined from the crystallographic analysis of the histone octamer (*61*) and the nucleosome (*52*). Also shown are the α-helical (gray) and *β*-sheet (checkered pattern) regions predicted from the primary structure of the protein (*36*). The numbers indicate the amino acid location in the sequences shown in (A).

with other core histones (histone octamer) and in the nucleosome.

MATERIALS AND METHODS

Protein Expression and Purification. Recombinant hTSH2B was expressed in *Escherichia coli* and purified as described previously (*28*).

Gel Electrophoresis. Sodium dodecyl sulfate (SDS)−polyacrylamide gel electrophoresis (PAGE) was performed as described by Laemmli (*29*). Two-dimensional gel electrophoresis was carried out as described elsewhere (*30*). Native 4.5% PAGE in 20 mM sodium acetate, 1 mM EDTA, and 40 mM Tris-HCl (pH 7.2) buffer for the analysis of nucleosome core particles was carried out according to Yager and van Holde (*31*). In some instances the buffer was changed to 0.5× TBE [45 mM Tris−borate, 1 mM EDTA (pH 8.3)]. Analysis of the restriction fragments in the nucleosome positioning experiments was carried out in 8% PAGE (20:1 acrylamide:bisacrylamide) and 8.3 M urea in 1× TBE [90 mM Tris−borate, 2 mM EDTA (pH 8.3)] as described in ref *32*. DNase I footprinting analysis was carried out in 8% PAGE (10:1 acrylamide:bisacrylamide) and 7 M urea in 1× TBE (*33*).

Circular Dichroism. Circular dichroism (CD) analysis of chicken histone H2B and hTSH2B in 100 mM NaCl and 10 mM Tris-HCl (pH 7.5) buffer was carried out at 20 °C. The spectra were recorded on a Jasco-J720 spectropolarimeter as previously described (*34*). The amount of α-helix was quantified as described in ref *35*.

Secondary Structure Prediction. The secondary structure of histones was predicted by SOPM (self-optimized prediction method) (*36*) available at the ExPASy Molecular Biology Server (http://au.expasy.org/).

Histone Octamer Reconstitution. Histone octamers were reconstituted from native chicken erythrocyte histones and FPLC-purified (*28*) recombinant hTSH2B following the procedure described in ref *37*. After reconstitution, the octamers were fractionated by gel filtration, in 2 M NaCl and 10 mM Tris-HCl (pH 7.5) buffer, using a 1.2 × 120 cm Sephacryl S-300-HR (see the Results section for more details).

Nucleosome Reconstitution. Recombinant human hTSH2B was mixed with chicken native H2A, H3, and H4 histones in stoichiometric amounts, and histone octamers were reconstituted onto either a random sequence 146 bp obtained from chicken erythrocyte nucleosome core particles (*33*) or onto a 196 bp fragment with defined sequence. The latter was obtained by *Eco*RI digestion of a 208−12 DNA construct consisting of 12 identical copies of a 196 bp fragment of the 5S rRNA gene from the sea urchin *Lytechinus variegatus* connected by a 12 bp DNA linker consisting of an *Eco*RI site at each end (*38*). After digestion with *Eco*RI, the 196 bp DNA was HPLC purified using a 75 × 7.5 mm Bio-Gel DEAE-5-PW (Bio-Rad, Hercules, CA). Reconstitution was carried out by a 2 to 0 M stepwise salt gradient dialysis (*39*) in 10 mM Tris-HCl (7.5) and 0.1 mM EDTA (8.0) as described elsewhere (*37*). The reconstituted chromatin particles thus obtained (at a concentration of ca. 40−50 μg/mL) were dialyzed against the appropriate buffers (*33*, *40*) and used for subsequent analytical ultracentrifuge analysis (*41*, *42*).

Sucrose Gradient Purification. Reconstituted hTSH2B nucleosome core particles in 10 mM Tris-HCl (pH 7.5) and 0.1 mM EDTA were loaded onto a 5−20% sucrose gradient in 25 mM NaCl, 10 mM Tris-HCl (pH 7.5), and 0.1 mM EDTA and centrifuged at 134400*g* for 19 h in a Beckman SW41 rotor at 4 °C. Fractions (0.5 mL) were collected and analyzed by SDS−PAGE.

Analytical Ultracentrifuge. Reconstituted hTSH2B nucleosomes were dialyzed against buffers of varying ionic strength as described in Ausió et al. (*33*). Sedimentation velocity runs were performed in a Beckman XL-A ultracentrifuge using an An-55 Al aluminum rotor. Samples were loaded in double-sector cells with aluminum-filled Epon centerpieces (*40*). UV scans were taken at 260 nm and analyzed by the van Holde and Weischet (*43*) method using the XL-A Ultra Scan version 4.1 sedimentation data software (Borries Demeler, Missoula, MT). A value of 0.650 cm^3/g was used for the partial specific volume of the nucleosome (*33*).

DNase I Footprinting. DNase I footprinting of reconstituted nucleosomes was carried out at 0 °C (*33*). γ-^{32}P-labeled nucleosomes at a concentration of approximately 0.14 μg/μL were digested with 0.1 unit/μL DNase I (Invitrogen)

(800 units of DNase I/mg of DNA). The digestion was carried out for 0, 5, 10, and 20 min in 12.5 mM NaCl, 4.5 mM Tris-HCl (pH 7.5), and 1 mM $MgCl_2$. The reaction was stopped by addition of EDTA to a final 25 mM and boiling for 1 min. Proteinase K (1.2 ng/μL) was then added, and the solution was incubated for 60 min at 37 °C. After digestion the samples were mixed with an equal volume of 98% deionized formamide, 0.4% bromophenol blue, 0.4% xylene cyanol, and 10 mM EDTA and loaded on 8% polyacrylamide sequencing gel containing urea. The dried gel was exposed overnight.

Nucleosome Positioning. The role of hTSH2B in the positioning of the nucleosome onto the 196 bp DNA fragment of the 5S rRNA gene of the sea urchin *L. variegatus* (*38*) was carried out as described elsewhere (*44*, *45*).

Histone H1 Binding. γ-^{32}P-labeled 196 bp nucleosomes were titrated with increasing amounts of chicken erythrocyte histone H1 as described in ref *46*. The electrophoretic mobility shift resulting from hisone H1 binding was analyzed by native 4.5% PAGE (see above).

Relaxation of Nucleosomes on DNA Minicircles. Nucleosome relaxation experiments were carried out as described previously using 351 and 356 bp pBR constructs (*47*).

RESULTS AND DISSCUSION

Histone hTSH2B Exhibits a Higher Helical Organization Than Histone H2B. The sequence of histone hTSH2B is shown in comparison to human H2B and chicken H2B (see Figure 1). Chicken H2B has been used in the experimental part of this work as a nonvariant counterpart to hTSH2B.

As shown in Figure 1A, the most significant primary structure difference between the main human/chicken somatic H2B variants and hTSH2B occurs at the N-terminal domain of the molecule. It involves only a limited number (nine) of amino acids in the N-terminal domain in addition to several (four) amino acid replacements throughout the rest of molecule that involve G → S, N → S, and N → T transitions. The limited extent of this variation would allow the classification of hTSH2B as a homeomorphous replacement histone variant (*48*, *49*).

The primary structure changes allow the prediction of a slight increase in the amount of secondary structure at the N-terminal end of hTSH2B (see Figure 1B). In fact, circular dichroism demonstrates a 6% increase in the α-helical content (Figure 2) as determined from the change in ellipticity at 222 nm (*50*). Careful inspection of the primary structure of hTSH2B (Figure 1A) shows that there is a replacement of two helix-breaker (proline) residues (present in both chicken and human somatic H2B) in the N-terminal domain of the hTSH2B. However, the predictive methods suggest that only an increase in β-turns occurs as a result of these substitutions (Figure 1B) and that the subtle increase in the α-helical content of this H2B variant may indeed occur in the histone fold.

The hTSH2B Reconstituted Histone Octamer Exhibits a Lower Stability Than the Chicken H2B Reconstituted Histone Octamer. Histone octamers were reconstituted using stoichiometric amounts of native chicken erythrocyte H2A, H3, and H4 and either native chicken H2B or hTSH2B, and the stability of the resulting complexes was assessed by gel filtration chromatography in 2 M NaCl (Figure 3) (*51*).

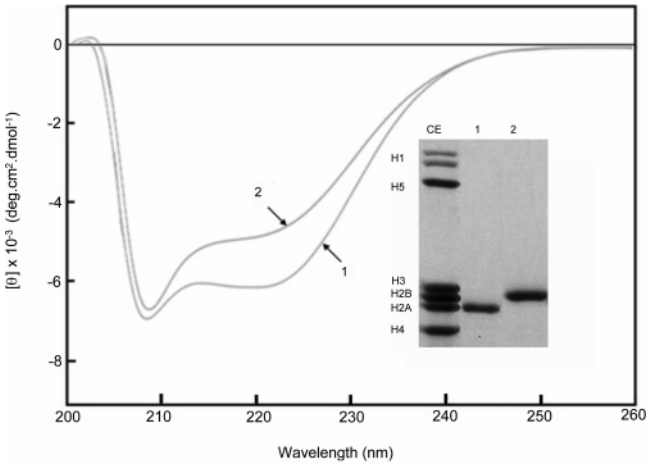

FIGURE 2: Circular dichroism spectra of histone H2B from chicken (line 2) in comparison to recombinant hTSH2B (line 1). The inset shows an SDS−PAGE of chicken hSTH2B (lane 1) in comparison to H2B (lane 2). CE is a chicken erythrocyte histone marker. Please note that hSTH2B comigrates with H2A on SDS−PAGE (*28*).

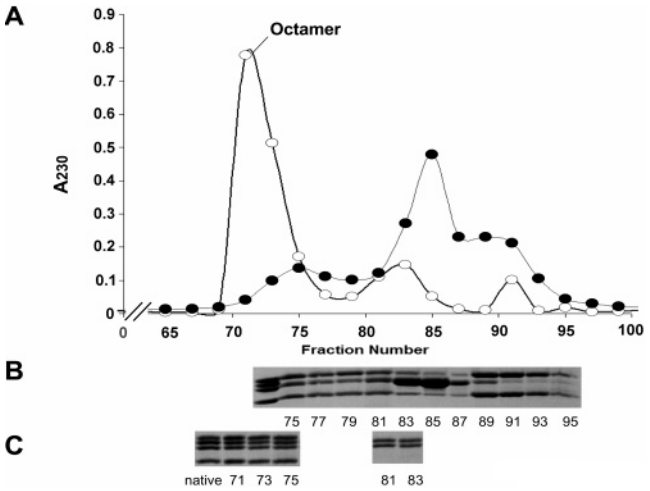

FIGURE 3: (A) Gel filtration chromatography of reconstituted histone octamer complexes using a Sephacryl S-300-HR resin on a 1.2 × 120 cm column eluted at 4 °C at 5 mL per four fractions per hour with 2 M NaCl and 10 mM Tris-HCl (pH 7.5) buffer. The black circles correspond to complexes reconstituted with hSTH2B, and the open circles correspond to complexes reconstituted from native histones. (B) and (C) are the SDS−PAGE electrophoretic analyses of some of the fractions corresponding to the hTSH2B (B) and native histone (C) reconstituted complexes, respectively. The numbers under the lanes are those of the fractions analyzed.

With the experimental protocol followed in this paper, histone octamers elute first, followed by H2A/H2B dimers and finally H3/H4 complexes (see Figure 3A,C). In 2 M NaCl, the native histone octamer [$(H3-H4)_2$ 2(H2A−H2B)] is in equilibrium with histone hexamers [$(H3-H4)_2$ (H2A−H2B)], tetramers [$(H3-H4)_2$], and dimers [(H2A−H2B)]. This equilibrium depends on the concentration of the starting sample, as well as on the pH and temperature (*51*).

As seen in Figure 3, while most of the complex reconstituted with native chicken histones elutes from the column as octamers, the histone complexes consisting of hTSH2B are eluted as a mixture in which the hTSH2B−H2A and H3−H4 complexes are the predominant forms. These results indicate that the hTSH2B-reconstituted histone complexes exhibit a reduced stability in 2 M NaCl at pH 7.5 and 4 °C

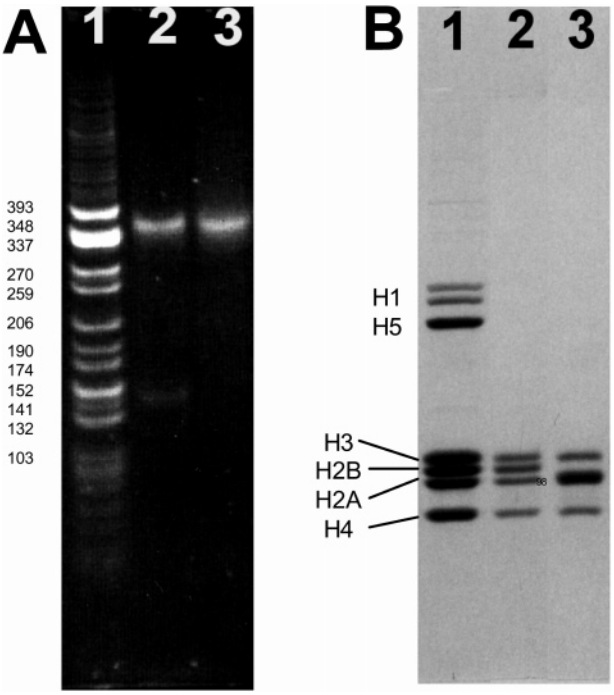

FIGURE 4: (A) Native 4.5% PAGE analysis of nucleosomes reconstituted with native histone octamers (lane 2) or with hSTH2B (lane 3). Lane 1 is a *Cfo*I cut pBR322 marker. The native gel was stained with ethidium bromide. (B) SDS−PAGE analysis of the histones from the reconstituted nucleosome core particles shown in (A). The assignment of lanes 2 and 3 is the same as in (A). Lane 1 is chicken erythrocyte histones used as a marker. The SDS−PAGE was stained with Coomassie blue.

when compared to the complexes consisting of the H2B counterpart. The interaction between the different histones is primarily determined by their histone fold domains. Within these regions, hTSH2B exihibits a sequence not unlike that for H2B (Figure 1). Therefore, in the absence of a crystallographic structure of the nucleosome (*52*, *53*) for this variant, it is difficult to establish the reasons for the observed lower stability of the hTSH2B-containing octamer. However, the possibility that this is the result of yet unclear interactions between the various core histone tails cannot be disregarded (*54*).

Association of Stoichiometric Amounts of hTSH2B, H2A, H3, and H4 with 146 bp DNA Produces Stable Nucleosome Core Particles. In contrast to the results described above, when stoichiometric amounts of histones in 2 M NaCl were mixed with 146 base pair random sequence DNA in the same salt concentration and sequentially dialyzed down to low ionic strength (*39*), nucleoprotein complexes were obtained that exhibit the same electrophoretic mobility in native gels as nNCP (Figure 4A). Furthermore, the reconstituted nucleoprotein complexes sedimented in sucrose gradients as nNCP (Figure 5A,B) and exhibited a stoichiometric histone composition (Figures 4B and 5C).

Sedimentation velocity analysis in the analytical ultracentrifuge confirmed these results (Figure 6). As seen in this figure, the sedimentation coefficient of the nucleosome core particles reconstituted from hTSH2B exhibits an ionic strength dependence very similar to that of the nucleosomes reconstituted with the native H2B counterpart or with nNCP themselves (*33*). Furthermore, the DNase I footprinting analysis (Figure 7) shows that hTSH2B-containing nucleosomes are structurally similar to nucleosomes reconstituted with the native H2B counterpart or nNCP.

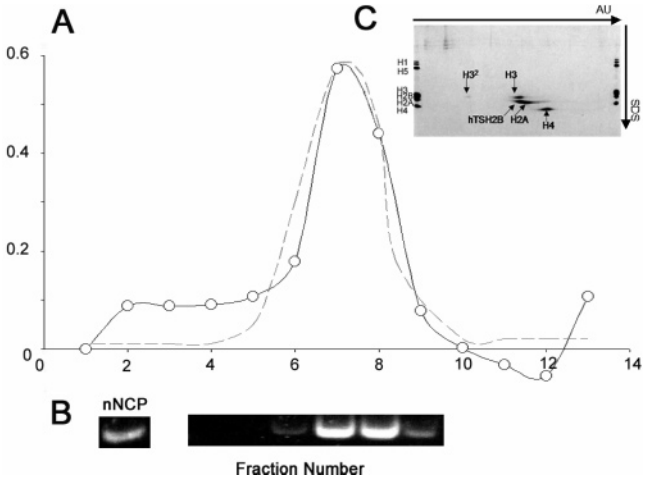

FIGURE 5: (A) Sucrose gradient fractionation of nucleosome core particles (NCPs). The solid line corresponds to hTSH2B-reconstituted NCPs, and the dashed line corresponds to chicken erythrocyte native NCPs. (B) Several fractions from the main peak were analyzed by native 4.5% PAGE and exhibited mobility identical to that of the *n*ative *n*ucleosome *c*ore *p*articles (nNCP) isolated from chicken erythrocyte chromatin. (C) Two-dimensional PAGE analysis of fractions 7 + 8. The first dimension was acetic acid−urea−PAGE (AU), and the second was SDS−PAGE (SDS).

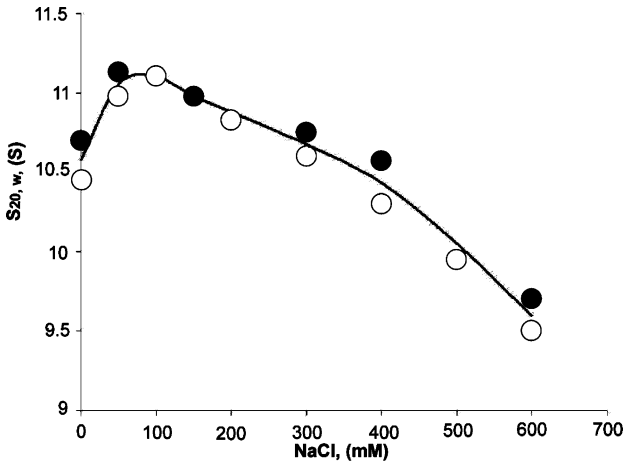

FIGURE 6: NaCl dependence of the sedimentation coefficient ($s_{20,w}$) of nucleosomes reconstituted with native histone octamers (open circles) or with hSTH2B (black circles). Sedimentation velocity experiments were carried out at 40000 rpm at 20 °C at different NaCl concentrations in 10 mM Tris-HCl and 0.1 mM EDTA (pH 7.5) buffer.

Histone hTSH2B Does Not Affect the Mobility of the Histone Octamer in the Nucleosome and Does Not Change the Nucleosomal DNA Topology nor Affects the Binding of Histone H1 to the Nucleosome. It has recently been shown that the nucleosomes consisting of histones bearing *sin* mutations and H2A.Z histone variants affect the mobility of the histone octamer (*55*). It has also been shown that the N-terminal tail of histone H2B plays a role in the sliding of histone octamers reconstituted onto linear DNA templates (*56*) and in the structural and dynamic polymorphism of nucleosomes reconstituted onto circular DNA templates (*47*). As the largest extent of variation in hTSH2B occurs at the N-terminal end of the molecule (Figure 1), we therefore decided to check whether any of these parameters are affected by the presence of this H2B variant.

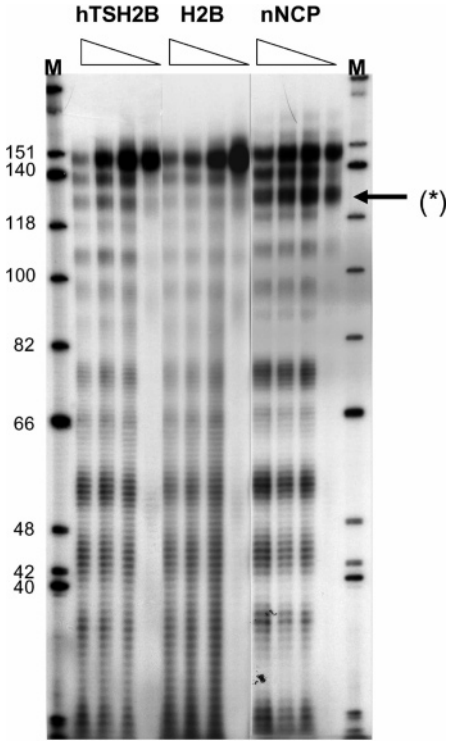

FIGURE 7: DNase I footprinting analysis of nucleosomes reconstituted with native histone (H2B) or with hTSH2B (hSTH2B) octamers, in comparison to chicken erythrocyte native nucleosome core particles (nNCP). The open triangles indicate the increasing time of digestion. M = ϕX174 *Hin*fI digested marker. The numbers on the left-hand side represent the base pair numbers. The asterisk on the right-hand side points to an artifact band in nNCP resulting from the occurrence of partial (ca. 125 bp) subnucleosome core particle contamination resulting from overdigestion of DNA during the process of nucleosome core particle preparation.

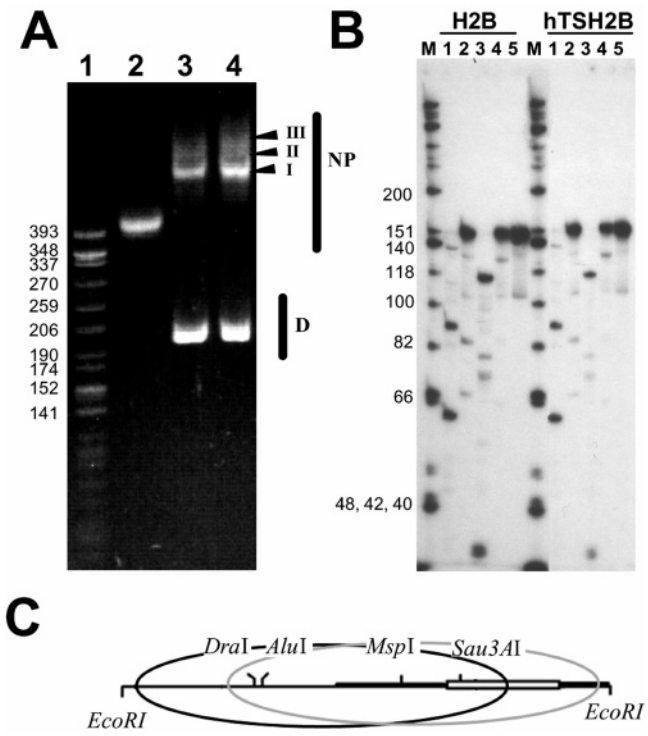

FIGURE 8: (A) Native 4.5% PAGE (0.5× TBE) analysis of nucleosomes reconstituted onto a 196 bp fragment of the 5S rRNA sea urchin gene using native H2B (lane 3) or hSTH2B (lane 4) reconstituted histone octamers in comparison to nNCP (lane 2). Lane 1 is a *Cfo*I cut pBR322 marker. The numbers on the left-hand side of the panel indicate the base pair size of the DNA fragments. The roman numerals point to different translational positions of the histone octamer. NP = nucleosome particle; D = free DNA. (B) Determination of the translational positioning of the native H2B and hSTH2B reconstituted nucleosomes on the 196 bp DNA fragment. The region of DNA directly associated with the histone octamer was determined by digestion of a gel-purified, end-labeled, deproteinized 146 bp micrococcal nuclease-resistant fragment with different restriction enzymes: *Dra*I (lane 1); *Alu*I (lane 2); *Msp*I (lane 3); *Sau*IIIA1 (lane 4). Lane 5 is the 146 bp micrococcal nuclease resistant undigested fragment. M = ϕX174 *Hin*fI digested marker. The numbers indicate the base pair size of the DNA fragments. (C) Schematic representation of the main translational nucleosome positions on the reconstituted 196 bp DNA fragment. The ellipsoid black line represents the predominant position, and a weaker position is depicted by the gray line ellipsoid. The heavy line indicates the 5S rRNA coding sequence, and the open box indicates the intragenic TFIIIA binding site.

To examine if nucleosome positioning was affected by the presence of the histone variant hSTH2B, nucleosomes were reconstituted onto a 196 bp DNA fragment of the 5S rRNA gene from the sea urchin *L. variegatus* (*38*). The nucleosome positioning was then compared to that of a nucleosome reconstituted on the same DNA template but consisting of native H2B. The results are shown in Figure 8. In native PAGE, both nucleosomes (see Figure 8A, lanes 3 and 4) appeared to consist of a major band and some minor bands with lower electrophoretic mobility (one for the native nucleosome and two for the variant nucleosome) corresponding to alternative positions. Incubation of these nucleosomes at different temperatures did not result in significant differences in this pattern (results not shown). A major and minor positioning was confirmed in both instances when the positioning was more accurately determined (Figure 8B; see also Figure 8C). The major position (approximately 90%) was found to be 5 ± 2 bp to 151 ± 2 bp, and the minor position (approximately 10%) was 47 ± 2 bp to 193 ± 2 bp (see Figure 8C) in agreement with previous results (*45*, *57*).

To assess whether hTSH2B would modulate nucleosome dynamics, nucleosomes were reconstituted onto 351 and 356 bp pBR DNA minicircles, relaxed with topoisomerase I, and the equilibrium products analyzed. When performed on a 351−366 bp minicircle series, this analysis has allowed one to determine the relative accessibility of minicircle-borne nucleosomes to three distinct conformations, depending on the path of the entry/exit DNAs: negatively or positively crossed and uncrossed (*47*). Data obtained with these two minicircle sizes were sufficient to conclude that hTSH2B- and regular H2B-containing nucleosomes were indistinguishable with respect to their respective conformational dynamics (results not shown).

Because of this lack of effect of the hTSH2B variant on the trajectory of the DNA entering and exiting the nucleosome, it was not surprising to find that binding of histone H1 (linker histones) to the nucleosome is not affected by the presence of hTSH2B. Gel shift analysis showed that H1 binds to the reconstituted nucleosomes with the same affinity and stoichiometry regardless of the presence or absence of hTSH2B (results not shown).

CONCLUDING REMARKS

Our results indicate that the human sperm histone variant hTSH2B can be reconstituted to form nucleosomes that

exhibit an almost identical structural conformation with nNCP. Thus, it is very likely that this variant exists in a nucleosome organization in the selected chromatin loci with which it appears to be associated within the human sperm nuclei (*28*).

It may be proposed that most of the structural effects associated to the chromatin regions enriched with TSH2B could be the result of posttranslational modifications, most likely phosphorylation at several sites that are unique to this variant (*28*). These modifications may affect the physical parameters (stability, dynamics) of the chemically modified nucleosome or create an alternative histone code.

The lack of stability of the hTSH2B histone octamer in the absence of DNA contrasts with the otherwise indistinguishable properties of nucleosome core particles reconstituted with these octamers. While this observation is puzzling, it is interesting to note that two of the mutations in hTSH2B at position 77 (G → S) and 86 (N → S) are in the histone fold domain and remarkably close to the Y → G *Sin* mutation at position 86 of yeast histone H2B. Importantly, this mutation has been shown to bypass the requirement for Swi-Snf in yeast (*58*). Thus, it is possible that the transitions observed in the histone fold of the variant H2B histone have a similar behavior.

ACKNOWLEDGMENT

We thank Ron M. Finn for skillful computer assistance in the preparation of the figures.

REFERENCES

1. Malik, H. S., and Henikoff, S. (2003) Phylogenomics of the nucleosome, *Nat. Struct. Biol. 10*, 882−891.
2. Ausió, J., and Abbott, D. W. (2002) The many tales of a tail: carboxyl-terminal tail heterogeneity specializes histone H2A variants for defined chromatin function, *Biochemistry 41*, 5945−5949.
3. Celeste, A., Difilippantonio, S., Difilippantonio, M. J., Fernandez-Capetillo, O., Pilch, D. R., Sedelnikova, O. A., Eckhaus, M., Ried, T., Bonner, W. M., and Nussenzweig, A. (2003) H2AX haploinsufficiency modifies genomic stability and tumor susceptibility, *Cell 114*, 371−383.
4. Bassing, C. H., Suh, H., Ferguson, D. O., Chua, K. F., Manis, J., Eckersdorff, M., Gleason, M., Bronson, R., Lee, C., and Alt, F. W. (2003) Histone H2AX: a dosage-dependent suppressor of oncogenic translocations and tumors, *Cell 114*, 359−370.
5. Mahadevaiah, S. K., Turner, J. M., Baudat, F., Rogakou, E. P., de Boer, P., Blanco-Rodriguez, J., Jasin, M., Keeney, S., Bonner, W. M., and Burgoyne, P. S. (2001) Recombinational DNA double-strand breaks in mice precede synapsis, *Nat. Genet. 27*, 271−276.
6. Lewis, J. D., Abbott, D. W., and Ausio, J. (2003) A haploid affair: core histone transitions during spermatogenesis, *Biochem. Cell Biol. 81*, 131−140.
7. Bonner, W. M. (2003) Low-dose radiation: thresholds, bystander effects, and adaptive responses, *Proc. Natl. Acad. Sci. U.S.A. 100*, 4973−4975.
8. Clarkson, M. J., Wells, J. R., Gibson, F., Saint, R., and Tremethick, D. J. (1999) Regions of variant histone His2AvD required for *Drosophila* development, *Nature 399*, 694−697.
9. Dryhurst, D., Thambirajah, A. A., and Ausió, J. (2004) New twist on H2A.Z: A histone variant with a controversial structural and functional past, *Biochem. Cell Biol. 82*, 490−497.
10. Park, Y.-J., Dyer, P. N., Tremethick, D. J., and Luger, K. (2004) A new fluorescence resonance energy transfer approach demonstrates that the histone variant H2A.Z stabilizes the histone octamer within the nucleosome, *J. Biol. Chem. 279*, 24274−24282.
11. Abbott, D. W., Ivanova, V. S., Wang, X., Bonner, W. M., and Ausió, J. (2001) Characterization of the stability and folding of H2A.Z chromatin particles: implications for transcriptional activation, *J. Biol. Chem. 276*, 41945−41949.
12. Meneghini, M. D., Wu, M., and Madhani, H. D. (2003) Conserved histone variant H2A.Z protects euchromatin from the ectopic spread of silent heterochromatin, *Cell 112*, 725−736.
13. Mizuguchi, G., Shen, X., Landry, J., Wu, W. H., Sen, S., and Wu, C. (2004) ATP-driven exchange of histone H2AZ variant catalyzed by SWR1 chromatin remodeling complex, *Science 303*, 343−348.
14. Krogan, N. J., Keogh, M. C., Datta, N., Sawa, C., Ryan, O. W., Ding, H., Haw, R. A., Pootoolal, J., Tong, A., Canadien, V., Richards, D. P., Wu, X., Emili, A., Hughes, T. R., Buratowski, S., and Greenblatt, J. F. (2003) A Snf2 family ATPase complex required for recruitment of the histone H2A variant Htz1, *Mol. Cell 12*, 1565−1576.
15. Pehrson, J. R., and Fried, V. A. (1992) MacroH2A, a core histone containing a large nonhistone region, *Science 257*, 1398−1400.
16. Abbott, D. W., Laszczak, M., Lewis, J. D., Su, H., Moore, S. C., Hills, M., Dimitrov, S., and Ausio, J. (2004) Structural characterization of macroH2A containing chromatin, *Biochemistry 43*, 1352−1359.
17. Changolkar, L. N., and Pehrson, J. R. (2002) Reconstitution of nucleosomes with histone macroH2A1.2, *Biochemistry 41*, 179−184.
18. Angelov, D., Molla, A., Perche, P. Y., Hans, F., Cote, J., Khochbin, S., Bouvet, P., and Dimitrov, S. (2003) The histone variant macroH2A interferes with transcription factor binding and SWI/SNF nucleosome remodeling, *Mol. Cell 11*, 1033−1041.
19. Ausió, J., and Abbott, D. W. (2004) in *Chromatin Structure and Dynamics* (Zlatanova, J., and Leuba, S. H., Eds.) Vol. 39, pp 249−290, Elsevier, Amsterdam, The Netherlands.
20. Palmer, D. K., O'Day, K., Trong, H. L., Charbonneau, H., and Margolis, R. L. (1991) Purification of the centromere-specific protein CENP-A and demonstration that it is a distinctive histone, *Proc. Natl. Acad. Sci. U.S.A. 88*, 3734−3738.
21. Lewis, J., Song, Y., de Jong, M., Bagha, S., and Ausió, J. (2003) A walk through vertebrate and invertebrate protamines, *Chromosoma 111*, 473−482.
22. Oliva, R., and Dixon, G. H. (1991) Vertebrate protamine genes and the histone-to-protamine replacement reaction, *Prog. Nucleic Acid Res. Mol. Biol. 40*, 25−94.
23. Meistrich, M. L., Brock, W. A., Grimes, S. R., Platz, R. D., and Hnilica, L. S. (1978) Nuclear protein transitions during spermatogenesis, *Fed. Proc. 37*, 2522−2525.
24. Churikov, D., Zalenskaya, I. A., and Zalensky, A. O. (2004) Male germline-specific histones in mouse and man, *Cytogenet. Genome Res. 105*, 203−214.
25. Gatewood, J. M., Cook, G. R., Balhorn, R., Schmid, C. W., and Bradbury, E. M. (1990) Isolation of four core histones from human sperm chromatin representing a minor subset of somatic histones, *J. Biol. Chem. 265*, 20662−20666.
26. Gusse, M., Sautiere, P., Belaiche, D., Martinage, A., Roux, C., Dadoune, J. P., and Chevaillier, P. (1986) Purification and characterization of nuclear basic proteins of human sperm, *Biochim. Biophys. Acta 884*, 124−134.
27. Tanphaichitr, N., Sobhon, P., Taluppeth, N., and Chalermisarachai, P. (1978) Basic nuclear proteins in testicular cells and ejaculated spermatozoa in man, *Exp. Cell Res. 117*, 347−356.
28. Zalensky, A. O., Siino, J. S., Gineitis, A. A., Zalenskaya, I. A., Tomilin, N. V., Yau, P., and Bradbury, E. M. (2002) Human testis/sperm-specific histone H2B (hTSH2B). Molecular cloning and characterization, *J. Biol. Chem. 277*, 43474−43480.
29. Laemmli, U. K. (1970) Cleavage of structural proteins during the assembly of the head of bacteriophage T4, *Nature 227*, 680−685.
30. Ausió, J. (1986) Structural variability and compositional homology of the protamine-like components of the sperm from bivalve molluscs, *Comp. Biochem. Physiol. 85B*, 439−449.
31. Yager, T. D., and van Holde, K. E. (1984) Dynamics and equilibria of nucleosomes at elevated ionic strength, *J. Biol. Chem. 259*, 4212−4222.
32. Howe, L., and Ausió, J. (1998) Nucleosome translational position, not histone acetylation, determines TFIIIA binding to nucleosomal *Xenopus laevis* 5S rRNA genes, *Mol. Cell. Biol. 18*, 1156−1162.
33. Ausió, J., Dong, F., and van Holde, K. E. (1989) Use of selectively trypsinized nucleosome core particles to analyze the role of the histone "tails" in the stabilization of the nucleosome, *J. Mol. Biol. 206*, 451−463.
34. Ausió, J., and van Holde, K. E. (1986) Histone hyperacetylation: its effects on nucleosome conformation and stability, *Biochemistry 25*, 1421−1428.

35. Wang, X., He, C., Moore, S. C., and Ausió, J. (2001) Effects of histone acetylation on the solubility and folding of the chromatin fiber, *J. Biol. Chem. 276*, 12764−12768.
36. Geourjon, C., and Deleage, G. (1994) SOPM: a self-optimized method for protein secondary structure prediction, *Protein Eng. 7*, 157−164.
37. Ausió, J., and Moore, S. C. (1998) Reconstitution of chromatin complexes from high-performance liquid chromatography-purified histones, *Methods 15*, 333−342.
38. Simpson, R. T., Thoma, F., and Brubaker, J. M. (1985) Chromatin reconstituted from tandemly repeated cloned DNA fragments and core histones: a model system for study of higher order structure, *Cell 42*, 799−808.
39. Tatchell, K., and van Holde, K. E. (1977) Reconstitution of chromatin core particles, *Biochemistry 16*, 5295−5303.
40. Garcia Ramirez, M., Dong, F., and Ausió, J. (1992) Role of the histone "tails" in the folding of oligonucleosomes depleted of histone H1, *J. Biol. Chem. 267*, 19587−19595.
41. Ausió, J., Seger, D., and Eisenberg, H. (1984) Nucleosome core particle stability and conformational change. Effect of temperature, particle and NaCl concentrations, and cross-linking of histone H3 sulfhydryl groups, *J. Mol. Biol. 176*, 77−104.
42. Ausió, J. (2000) Analytical ultracentrifugation and the characterization of chromatin structure, *Biophys. Chem. 86*, 141−153.
43. van Holde, K. E., and Weischet, W. O. (1978) Boundary analysis of sedimentation velocity experiments with monodisperse and paucidisperse solutes, *Biopolymers 17*, 1387−1403.
44. Dong, F., Hansen, J. C., and van Holde, K. E. (1990) DNA and protein determinants of nucleosome positioning on sea urchin 5S rRNA gene sequences *in vitro*, *Proc. Natl. Acad. Sci. U.S.A. 87*, 5724−5728.
45. Howe, L., Iskandar, M., and Ausió, J. (1998) Folding of chromatin in the presence of heterogeneous histone H1 binding to nucleosomes, *J. Biol. Chem. 273*, 11625−11629.
46. Howe, L., Itoh, T., Katagiri, C., and Ausió, J. (1998) Histone H1 binding does not inhibit transcription of nucleosomal *Xenopus laevis* somatic 5S rRNA templates, *Biochemistry 37*, 7077−7082.
47. Sivolob, A., Lavelle, C., and Prunell, A. (2003) Sequence-dependent nucleosome structural and dynamic polymorphism. Potential involvement of histone H2B N-terminal tail proximal domain, *J. Mol. Biol. 326*, 49−63.
48. Ausió, J., Abbott, D. W., Wang, X., and Moore, S. C. (2001) Histone variants and histone modifications: a structural perspective, *Biochem. Cell. Biol. 79*, 693−708.
49. West, M. H., and Bonner, W. M. (1980) Histone 2A, a heteromorphous family of eight protein species, *Biochemistry 19*, 3238−3245.
50. Bradbury, E. M., Cary, P. D., Crane-Robinson, C., Rattle, H. W., Boublik, M., and Sautiere, P. (1975) Conformations and interactions of histone H2A (F2A2, ALK), *Biochemistry 14*, 1876−1885.
51. Eickbush, T. H., and Moudrianakis, E. N. (1978) The histone core complex: an octamer assembled by two sets of protein−protein interactions, *Biochemistry 17*, 4955−4964.
52. Luger, K., Mader, A. W., Richmond, R. K., Sargent, D. F., and Richmond, T. J. (1997) Crystal structure of the nucleosome core particle at 2.8 Å resolution, *Nature 389*, 251−260.
53. Suto, R. K., Clarkson, M. J., Tremethick, D. J., and Luger, K. (2000) Crystal structure of a nucleosome core particle containing the variant histone H2A.Z, *Nat. Struct. Biol. 7*, 1121−1124.
54. Hansen, J. C., Tse, C., and Wolffe, A. P. (1998) Structure and function of the core histone N-termini: more than meets the eye, *Biochemistry 37*, 17637−17641.
55. Flaus, A., Rencurel, C., Ferreira, H., Wiechens, N., and Owen-Hughes, T. (2004) Sin mutations alter inherent nucleosome mobility, *EMBO J. 23*, 343−353.
56. Hamiche, A., Kang, J. G., Dennis, C., Xiao, H., and Wu, C. (2001) Histone tails modulate nucleosome mobility and regulate ATP-dependent nucleosome sliding by NURF, *Proc. Natl. Acad. Sci. U.S.A. 98*, 14316−14321.
57. Meersseman, G., Pennings, S., and Bradbury, E. M. (1991) Chromatosome positioning on assembled long chromatin. Linker histones affect nucleosome placement on 5 S rDNA, *J. Mol. Biol. 220*, 89−100.
58. Recht, J., and Osley, M. A. (1999) Mutations in both the structured domain and N-terminus of histone H2B bypass the requirement for Swi-Snf in yeast, *EMBO J. 18*, 229−240.
59. Ohe, Y., Hayashi, H., and Iwai, K. (1979) Human spleen histone H2B. Isolation and amino acid sequence, *J. Biochem. 85*, 615−624.
60. Grandy, D. K., Engel, J. D., and Dodgson, J. B. (1982) Complete nucleotide sequence of a chicken H2b histone gene, *J. Biol. Chem. 257*, 8577−8580.
61. Arents, G., Burlingame, R. W., Wang, B. C., Love, W. E., and Moudrianakis, E. N. (1991) The nucleosomal core histone octamer at 3.1 Å resolution: a tripartite protein assembly and a left-handed superhelix, *Proc. Natl. Acad. Sci. U.S.A. 88*, 10148−10152.

BI048061N